Geosci. Instrum. Method. Data Syst. Discuss., https://doi.org/10.5194/gi-2019-8
Manuscript under review for journal Geosci. Instrum. Method. Data Syst.
Discussion started: 3 April 2019

Geoscientific Instrumentation Methods and Data Systems Discussions
Open Access
EGU

A user-orientated column modelling framework for efficient analyses of the Martian atmosphere

Mark Paton[1], Ari-Matti Harri[1], Oliver Vierkens[1], and Hannu Savijärvi[2]
[1]Finnish Meteorological Institute, PO Box 503, FIN-00101 Helsinki, Finland
[2]Department of Physics, University of Helsinki, FI-00560, Finland
Correspondence to: Mark Paton (mark.paton@fmi.fi)

Abstract.

As spacecraft missions return ever more data from Mars additional tools will be required to explore and analyse these datasets efficiently. To streamline research into the atmosphere of Mars a user-orientated modelling capability is developed that enables automatic initialisation and running of a column model.

As a demonstration we utilise the modelling framework to provide additional verification for the University of Helsinki/Finnish Meteorological Institute Mars column model temperature profiles at the higher altitudes. We utilise the framework at well characterised landing sites to understand the model's applicability and to identify future opportunities for modifications to the framework. We do this by using the framework to compare the column model to temperature soundings made by Mars Reconaissance Orbiter.

We find the column model is able to reproduce the observed lapse rates and average temperatures closely in most cases except for a 20-60 K increase over the northern hemisphere mid-winter. By incorporating an adiabatic heating term into the column model we suggest this discrepancy is likely due to the adiabatic compression of down welling air. We estimate maximum downward vertical velocities at the VL-1 and VL-2 latitudes of 8 and 12 cm s^{-1} at altitudes of 15 and 20 km respectively over the winter solstice. The fitting approach developed here provides a way to independantly estimate or 'observe' the vertical motion in the Martian atmosphere.

We have introduced new application software that can quickly find and display the requested data and can be immediately analysed using the included tools. We have demonstrated the potential of this software application with a glimpse into the upper atmosphere of Mars and identified future modifications to the framework.

Geosci. Instrum. Method. Data Syst. Discuss., https://doi.org/10.5194/gi-2019-8
Manuscript under review for journal Geosci. Instrum. Method. Data Syst.
Discussion started: 3 April 2019

Geoscientific Instrumentation Methods and Data Systems Discussions
Open Access
EGU

1 Introduction

Observational data is being returned from Mars in ever increasingly quantities by spacecraft. To manipulate this data and compare it with the vast amounts of data generated by computer models specialised software tools are required. Tools for searching, extracting and visualising the relevant data have been made readily available by the space agencies. Exploration of these large datasets, if stored online, can be time consuming and important data may be missed due to time constraints. Ideally the data needs to be stored on a host machine and accessible via a local network with a fast connection or to be stored on the same work station that being used for analysis. This then requires the integration of tools to query the database and analyse the data into a single package.

Column models of the Martian atmosphere are a fast and convenient analytical tool for investigating the lower sections of the Martian atmosphere. With a suitable radiation scheme they can accurately model the temperature in the lower part of the atmosphere (Savijärvi et al., 2005). A 1D model can be particularly well suited to investigating the Martian atmosphere at specific locations such as landing sites. This is because the radiative timescale of the atmosphere (1-2 sols) is short, making it relatively insensitive, compared to Earth's atmosphere, to horizontal heat transfer through advection.

At particular times of year and at certain locations the atmosphere deviates from radiative equilibrium e.g. during the northern hemisphere winter, as warm air is generated by adiabatic compression of descending arm of the meridional circulation (Heavens et al., 2011). This can create a significant temperature inversion up to an altitude of between 10 and 20 km at mid to high latitudes. The magnitude of this temperature inversion may be controlled, to some degree, by radiative forcing from atmospheric dust. When using a column model care then needs to be taken to make sure any large-scale dynamical processes are not interfering with the interpretation of the results from the model. Alternatively a term could be included in the model to account for the adiabatic heating.

In the next section we describe a column model and satellite soundings in the Martian atmosphere. In section 3 we give a system level overview of the software application and describe its operation. In addition we introduce an adiabatic heating adjustment for the model. In section 4 we demonstrate the use of the application and verify the column model. In section 5 we discuss the reasons for differences between the column model results and the soundings. Tables of the times, location, thermal inertia and albedo for individual vertical profiles can be found in the appendix.

2 Background

The University of Helsinki and Finnish Meteorological Institute (UH/FMI) have developed a column model that has been extensively used to investigate the Planetary Boundary Layer at Mars including surface-atmosphere interactions (Savijärvi et al., 2004; Savijärvi, 1999; Savijärvi and Kauhanen, 2008; Savijärvi and Määttänen, 2010; Savijärvi et al., 2005; Savijärvi, 1995; Paton et al., 2016;

Geosci. Instrum. Method. Data Syst. Discuss., https://doi.org/10.5194/gi-2019-8
Manuscript under review for journal Geosci. Instrum. Method. Data Syst.
Discussion started: 3 April 2019

Geoscientific Instrumentation Methods and Data Systems Discussions
Open Access
EGU

Savijärvi et al., 2018). The model includes time-stepping calculations for wind, temperature, specific humidity and ice mixing ratio. It includes long and short wave radiation schemes taking into account atmospheric CO2-H2O and dust. For turbulence a Monin-Obukhov scheme is used for the lowest layer and a mixing approach aloft. Energy balance at the surface uses a Crank-Nicholson method to calculate the surface temperature. Surface ice and adsorption is also modelled.

Soundings by orbiting spacecraft, which consist of vertical profiles of atmospheric properties, are used to observe and characterise the atmosphere. These can be combined to build a picture over large regions and time periods. The Mars Climate Sounder (MCS) aboard the Mars Reconnaissance Orbiter has been observing the temperature, humidity and dust content of the Martian atmosphere from 2006 onward. The instrument views Mars through eight thermal infrared channels and one spectral channel with a total of 21 detectors (Joyner and Sayfi, 2012; McCleese et al., 2007). The standard viewing strategy for MCS is to observe along its direction of travel from a frozen orbit with an inclination of 92°. Limb and nadir observations are made in succession during each sounding acquisition with the nadir observation providing near surface information on the atmosphere with a vertical resolution of about 1 km. The frozen orbit enables MCS to acquire one morning and early afternoon sounding from each latitude and longitude on Mars. Horizontal resolution for the nadir observations are 1.7 km along the direction of travel.

3 Method

3.1 Description and operation of the framework

A Python-based wrapper has been designed to search MCS data using a filter, initialising the column model with MCS data and other observational input, running the model and displaying the results together with the MCS data. The filter uses location, time of day and season as search parameters which can be entered via a Graphical User Interface (GUI). The model is initialised with automatically retrieved TES thermal inertia and albedo values using the location retrieved from the heading for each sounding extracted from the MCS data. The model is initialised at midnight for the solar longitude (Ls) of the MCS sounding and run for 5 sols. Surface pressure and temperature are initialised in this way too.

Figure 2 shows the software components, files and data flow used in the application. As can be seen the Python code interacts with the column model through intermediate initialisation and output files.

The 1D column model can then be automatically run by the code at the specified location and then the resulting temperature profile can be compared to the MCS temperature profile at the local time of the sounding. The comparison is made by finding the best fit of the column model to the temperature sounding. This is done by first calculating the average temperatures for both the observed profile and model profile.

Geosci. Instrum. Method. Data Syst. Discuss., https://doi.org/10.5194/gi-2019-8
Manuscript under review for journal Geosci. Instrum. Method. Data Syst.
Discussion started: 3 April 2019

Geoscientific Instrumentation Methods and Data Systems Discussions
Open Access
EGU

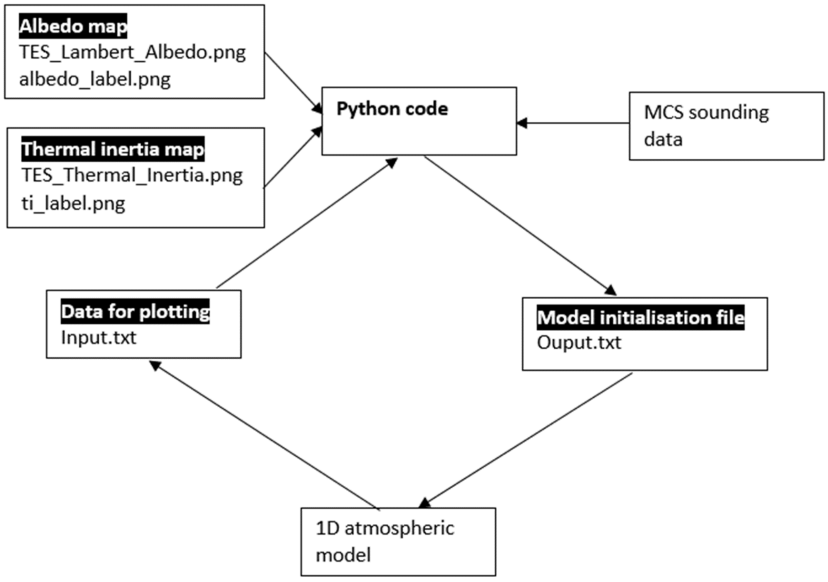

Fig. 1. Software, files and data paths used by the application.

The code is organised into three components as shown in figure 3. One component contains the GUIs and performs the basic operations activated by the GUI. Another component contains the data processing and analysis tools required for performing the main functions of the applications. The third component contains the database tools for fetching and storing the data for easy access by the application. The database framework also allows easy expansion of the database.

Geosci. Instrum. Method. Data Syst. Discuss., https://doi.org/10.5194/gi-2019-8
Manuscript under review for journal Geosci. Instrum. Method. Data Syst.
Discussion started: 3 April 2019

Geoscientific Instrumentation Methods and Data Systems Discussions

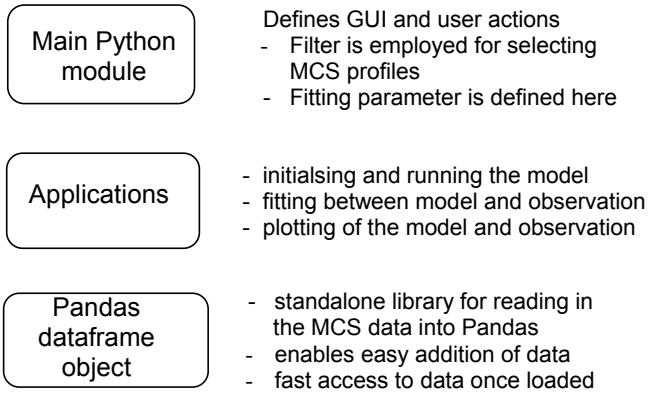

Fig. 2. Organisation of the code into three main sections.

3.2 Adiabatic heating modification for the column model

Column models do not as such provide vertical motion. For the present application, a simple but realistic approximation of adiabatic heating (Holton, 2004) due to the systematic downward motion in the meridional Hadley cell, was added to the model. Its temperature tendency equation then reads (with horizontal advections omitted)

$$\frac{\partial Q}{\partial t} = -w(\Gamma_d - \Gamma) + Q_{rad} + Q_{turb} \tag{1}$$

where $\Gamma = -dt/dz$ is the actual temperature lapse rate (by finite difference at each time step and altitude point), and Γ_d is the constant adiabatic lapse rate, 5 K/km on Mars. The other r.h.s terms are due to radiation and turbulence. Vertical velocity $w(z)$ must now be provided as an extra parameter.

The assumed structure used to represent a typical profile of the vertical wind (see Fig. 9) is based on a parabolic function for the upper part and the formula for a circle on the lower section.

$$w_{top} = -f_z \frac{v_z - v_l}{400} \frac{z(j) - z_l}{1000} \left[f_z \frac{z(j) - z_l}{1000} - 40 \right] \tag{2}$$

where f_z is a factor that controls the width, i.e. vertical distance between the two arms, of the parabolic function, v_z is the maximum vertical wind speed, v_l is the vertical wind speed at which point w_{low} function (see below) begins or is 'linked' to w_{top} and z_l is the altitude at which w_{low} begins.

$$w_{low} = v_l - v_l \left[1 - \frac{z(j)^2}{z_l^2} \right]^{0.5} \tag{3}$$

The fit parameter for comparing the modified model to the soundings is calculated as follows:

$$T_f^2 = \sum_{n=1}^{5} (T_n - S_n)^2 \tag{4}$$

Geosci. Instrum. Method. Data Syst. Discuss., https://doi.org/10.5194/gi-2019-8
Manuscript under review for journal Geosci. Instrum. Method. Data Syst.
Discussion started: 3 April 2019

Geoscientific Instrumentation Methods and Data Systems Discussions
Open Access
EGU

where T_n is the temperature from the model, S_n is the temperature from the MCS sounding and n is the index for the altitude of the temperature. The model and observations are compared at the model altitude levels of 7000, 10000, 14000, 20000 and 28000 m corresponding to index numbers n=1, 2, 3, 4 and 5 respectively. A hill climbing algorithm was used to vary the profile coefficients f_z,v_z,v_l and z_l once each sol. The column model repeated the temperature calculation for the sol until T_f was below a predefined threshold that was set taking into account accuracy and running time constraints. The threshold temperature was set at 3 K giving a fitting error of around 1-2 K for each point.

The column model was spun-up over four sols to enable the upper atmosphere to reach equilibrium. The sol used for fitting was then the fifth sol.

4 Verification of the column model

The column model is first verified, without the adiabatic heating adjustment, by comparing it to soundings made by MCS. The MCS data was searched for soundings around the VL-1 landing site (22.5°N, 50°W) using the new tool described in section 3 in order to check the MCD (Lewis et al., 1999) data and compare with our column model. The parameters used for the search were longitude, latitude, solar longitude and local time with the ranges of -53° to -43°, 17° to 27° for longitude and latitude. For solar longitude the range was searched between LS±10° and LTST 0 to 0.25 for morning soundings and 0.25 to 1.0 for afternoon soundings. The values for opacity were estimated from MCD, thereby taking into account seasonal and areal distributions in dust. Values of 0.4 were estimated for VL-1, VL-2 and MSL except during the northern winter solstice when a value of 1.0 was used for VL-1 and MSL.

Figures 3 to 6 show the temperatures retrieved from the sounding data together with the column model, which was initialised with information specific for each case as described in section 2.2. Overlaying the figures are climate model temperatures from the MCD.

The model was initialised with thermal inertia and albedo from TES maps. These were read using the coordinates of the profile supplied with each sounding header in the MCS data. Likewise with the surface temperature and pressure. Many of the soundings do not reach the surface as the lower segments of the profile are rejected due to the various selection criteria used to judge a successful retrieval (Kleinböhl et al., 2009). Tables listing times, location, thermal inertia, albedo for each sounding used can be found in the appendix.

Geosci. Instrum. Method. Data Syst. Discuss., https://doi.org/10.5194/gi-2019-8
Manuscript under review for journal Geosci. Instrum. Method. Data Syst.
Discussion started: 3 April 2019

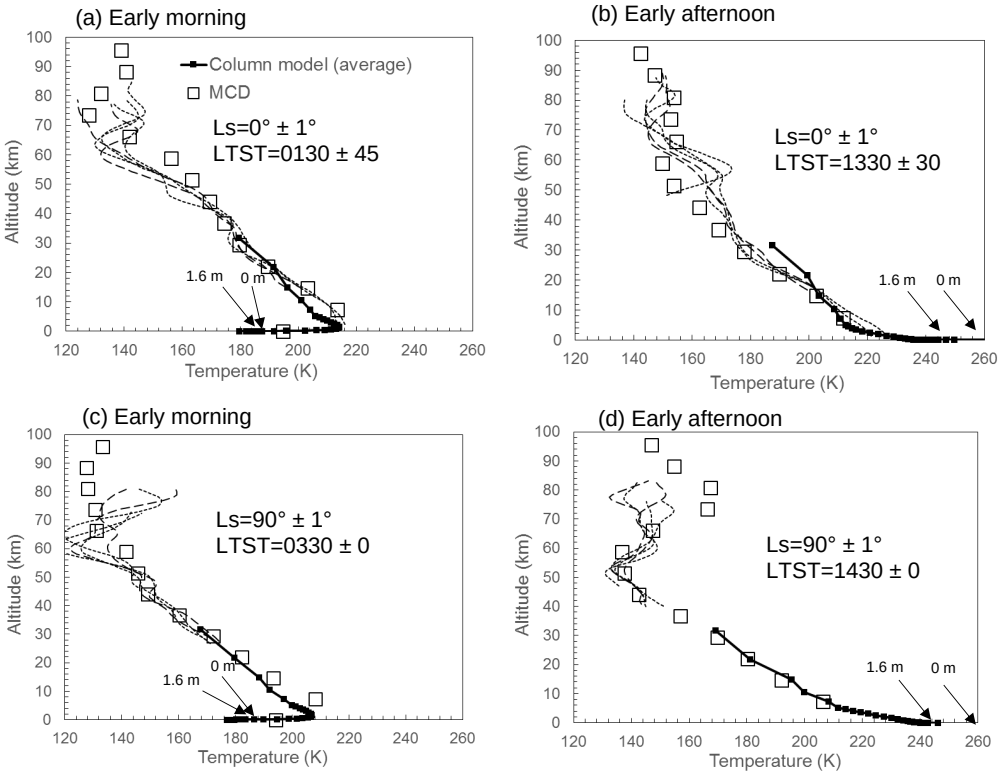

Fig. 3. Viking Lander 1 site temperatures observed by the Mars Climate Sounder together with temperatures from the column model. Five MCS soundings are plotted in each figure. The profile locations range from latitudes between 17° and 27°N and longitudes between 43° and 53°W. The range of solar longitudes and local times are indicated in the legends for each set of profiles. Early morning and afternoon profiles are plotted for the spring equinox and the summer solstice. Plots for subsequent seasons can be found in the next figure. Also shown are the VL-1 1.6 m altitude temperature measurements and inferred surface temperature from Paton et al. (2016). Overlaid, as a check, is data from the MCD. see the appendix for a table listing details of each sounding and input data for the model.

Geosci. Instrum. Method. Data Syst. Discuss., https://doi.org/10.5194/gi-2019-8
Manuscript under review for journal Geosci. Instrum. Method. Data Syst.
Discussion started: 3 April 2019

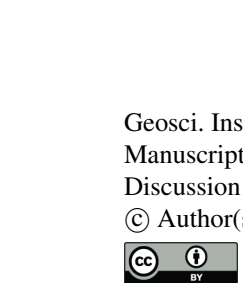

Geoscientific Instrumentation Methods and Data Systems Discussions
Open Access
EGU

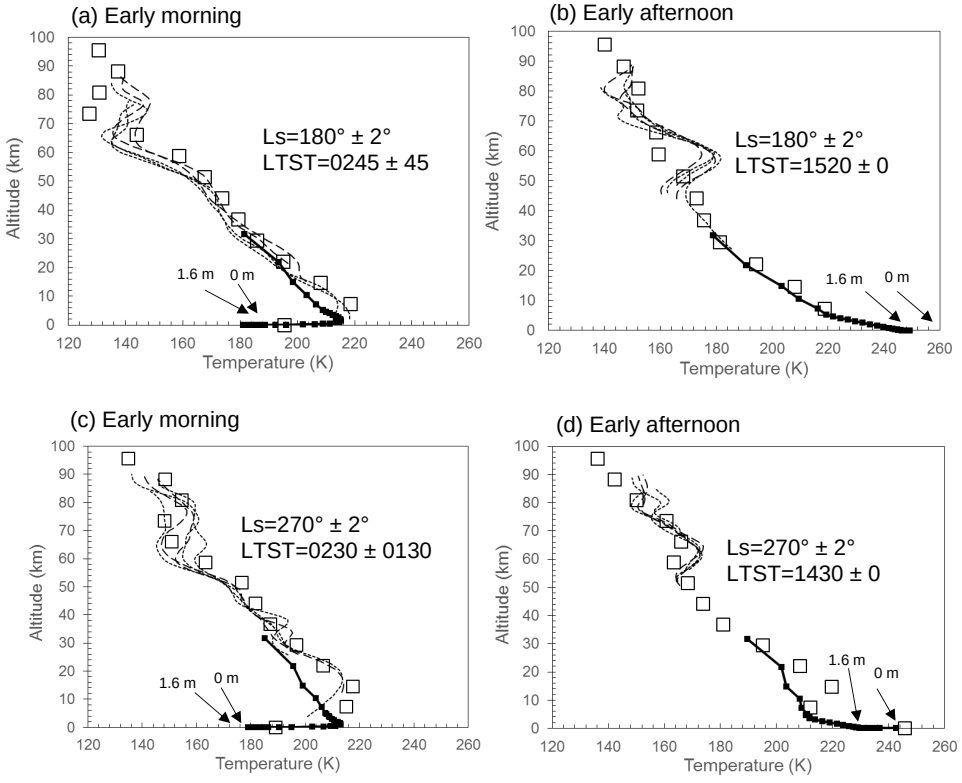

Fig. 4. VL-1 site MCS temperature soundings and model temperatures compared. As Fig. 3 but for the autumn equinox (Ls 180°) and the winter solstice (Ls 270°). Five MCS soundings are plotted in each figure. See the previous figure caption for preceding seasons and details regarding the profiles locations and an explanation of the legends. Also shown are the 1.6 m altitude temperature measurements and inferred surface temperature from Paton et al. (2016). Overlaid, as a check, is data from the MCD.

Geosci. Instrum. Method. Data Syst. Discuss., https://doi.org/10.5194/gi-2019-8
Manuscript under review for journal Geosci. Instrum. Method. Data Syst.
Discussion started: 3 April 2019

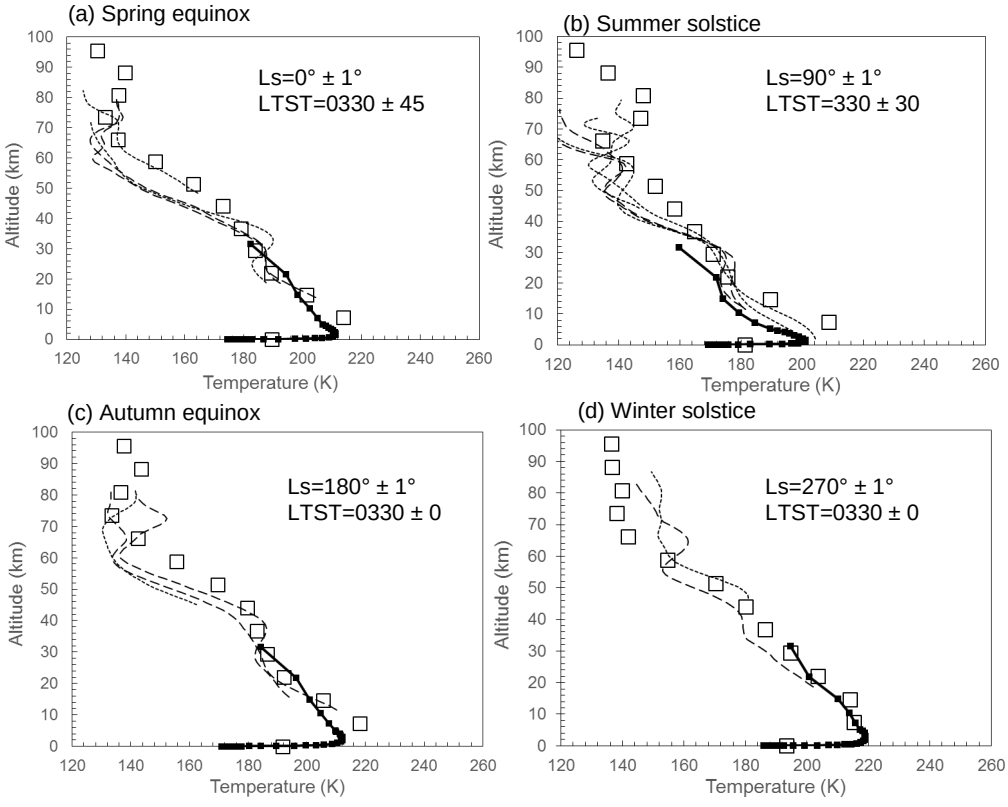

Fig. 5. Temperatures observed by the Mars Climate Sounder together with temperatures from the column model. Overlaid, as a check, is data from the MCD. The location is around Gale Crater. As Figs. 3-4, but for the MSL site (4.6°S, 137.4°E)

Geosci. Instrum. Method. Data Syst. Discuss., https://doi.org/10.5194/gi-2019-8
Manuscript under review for journal Geosci. Instrum. Method. Data Syst.
Discussion started: 3 April 2019

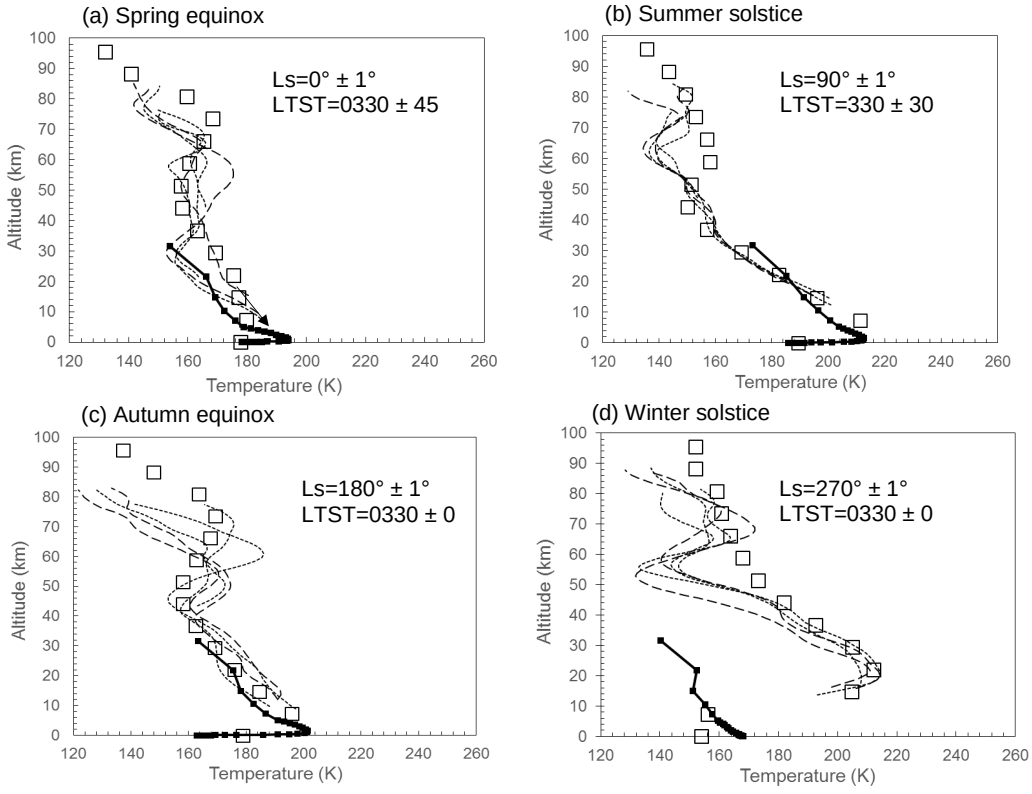

Fig. 6. Temperatures observed by the Mars Climate Sounder together with temperatures from the column model. Five MCS soundings are plotted in each figure. Overlaid, as a check, is data from the MCD. The location is around the VL-2 site. As Figs. 3-4, but for the VL-2 site (48.0°N, 134.3°E)

Geosci. Instrum. Method. Data Syst. Discuss., https://doi.org/10.5194/gi-2019-8
Manuscript under review for journal Geosci. Instrum. Method. Data Syst.
Discussion started: 3 April 2019

The MCS temperature soundings in figures 3 to 6 are somewhat similar to each other despite being retrieved over a large region, with diverse surface properties, surrounding each landing site. The similarity in temperature profiles above about 10 km is consistent with GCM results and observations that suggest the temperature in this region of the atmosphere is largely controlled by the large-scale circulation of the climate. Below 10 km, in situ wind meaurements (Paton et al., 2018), also indicate good agreement with GCM results in terms of wind direction perhaps reflecting the influence of the large scale circulation. However wind speed is less consistent with GCM results, perhaps reflecting some local influences from variations in topography or surface thermal properties at these altitudes.

Due to the lack of full coverage down to the surface from MCS it is difficult to compare individual plots to each other. It is apparent though that column model, soundings and MCD are in broad agreement with the observations. Both the soundings and the MCD tend to be slightly warmer than the column model in the lowest 10 km. At Ls=270° the MCD is significantly warmer than the column model.

While the column model satisfactorily reproduces the majority of the temperature profiles observed by MCS large differences are clearly apparent at the VL-1 and VL-2 sites around the winter solstice in figures 4 (c) and 6 (d) respectively. The maximum temperature difference is 20 K at an altitude of 15 km at the VL-1 site. Even larger temperature differences occur over the VL-2 reaching a maximum of 60 K at an altitude of 20 km. The column model matches the MCS observations satisfactorily over the entire Martian year. at the MSL site, however.

There is some disagreement between the surface temperature from the column model and the near surface Viking lander measurements with the MCD. The surface temperature of the MCD appears to be 10-20 K warmer than the column model and the near-surface measurements in nearly all cases. The only close agreements occur at the VL-2 sites over the spring equinox and summer solstice.

The disagreement with the MCD may not be surprising. GCMs cannot reproduce strong night-time temperature inversions (Lewis et al., 1999) and so may produce warmer temperatures during the night. This seems to bear out when comparing the night-time temperatures at the VL-1 and VL-2 sites over the spring equinox and summer solstice. At the VL-2 site the lander measurements closely match the MCD temperatures. The MCD also agrees with the column model which also suggest a weaker night-time temperature inversion than at the VL-1 site. Also there may be some unaccounted surface heterogeneity that cannot be resolved by the large grid size of a GCM, i.e. about 200 km for the LMD model used for generating MCD data. In general climate and mesoscale models are in error of -10 to 10 K from lander measurements (Spiga and Forget, 2009; Rafkin et al., 2001; Tyler et al., 2002; Toigo and Richardson, 2002)

Geosci. Instrum. Method. Data Syst. Discuss., https://doi.org/10.5194/gi-2019-8
Manuscript under review for journal Geosci. Instrum. Method. Data Syst.
Discussion started: 3 April 2019

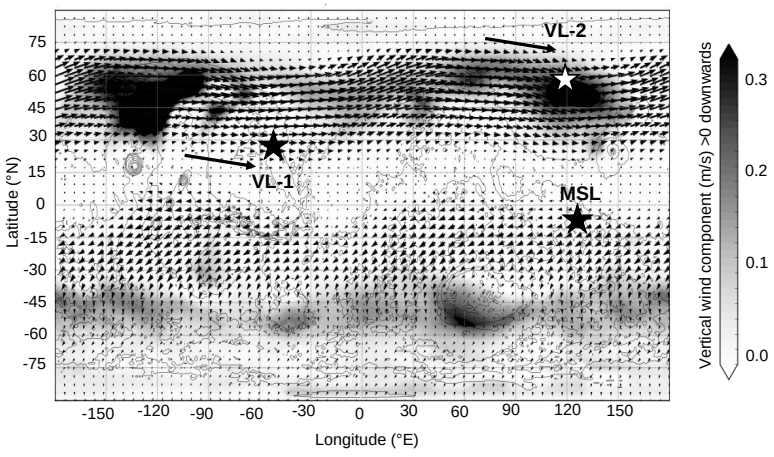

Fig. 7. MCD vertical velocity w and horizontal winds at an altitude of 20 km. Note to make visualisation of the down welling regions clearer only the positive down welling velocity is shown. Any negative velocities are white. The long arrows next to the VL-1 and VL-2 sites represent the direction of the winds immediately to the west of those sites.

5 Atmospheric circulation probed with the column model

In the previous section we found good agreement between the model and the temperature soundings at the spring equinox, summer solstice and autumn equinox. The observed temperature at the winter solstice was found to be significantly warmer than the column model by up to 20 K and 60 K at the VL-1 and VL-2 sites respectively. Warming of the atmosphere by this amount has been reproduced in climate models suggesting large departures from radiative equilibrium. The warming is thought to be the heating from adiabatic compression of the atmosphere from the systematic downward motion of the air due to the seasonal meridional circulation (Heavens et al., 2011).

Figure 7 shows the location of the landing sites for VL-1, VL-2 and MSL in relation to the down welling regions and the horizontal winds at 20 km height which meander around Mars as planetary waves (Read and Lewis, 2004). The down welling branch in the northern hemisphere varies in intensity longitudinally. This is due to longitudinal variations in topography and surface thermal properties. For example variations in topography tends to modify the flow concentrating it into currents, i.e. Western Boundary Currents that flow down the flanks of Tharsis and Syrtis.

To reproduce the atmospheric heating at the latitudes of the VL-1 and VL-2 site we can add an adiabatic heating term as described in section 3 to the column model. As can be seen in figures 8 (a) and (b) there is a significant improvement in the agreement between the model and the soundings when adding an adiabatic heating term. The fitting parameter together with the parameters for the shape of the vertical wind profile can be found in section 3. By fitting the model temperature profile to the soundings then, in principle, the vertical wind speed at each site can be estimated. However the atmospheric temperature over each site will also be heated or cooled by advected air masses due to the strong westerlies at the VL-1 and VL-2 latitudes.

Geosci. Instrum. Method. Data Syst. Discuss., https://doi.org/10.5194/gi-2019-8
Manuscript under review for journal Geosci. Instrum. Method. Data Syst.
Discussion started: 3 April 2019

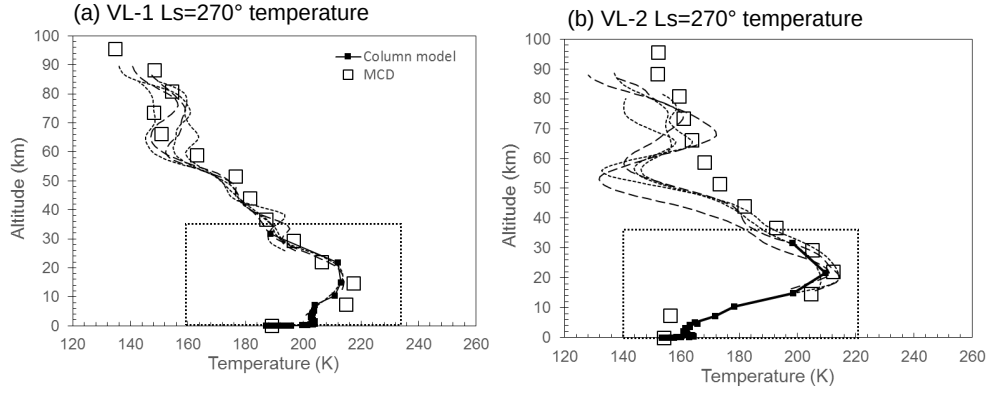

Fig. 8. Fit of the column model to the soundings at Ls=270° using the adjustment for adiabatic heating found in section 3. The boxes in each figure please refer to figure 9.

Figures 9 (a) and (b) compares the resulting vertical wind profile from fitting the column model with MCD data. As indicated in section 2.3 the vertical wind profile in the model is kept constant throughout the entire sol and varied after each sol to obtain a fit of the model to the sounding. This is because we are interested in influences from large-scale processes, such as advection, on the local environment. There is some diurnal variation in the vertical wind profile, by going by its periodicy, we assume to be caused by more local influences on the atmosphere.

Included on each plot is a zonally sol averaged profile created from MCD data. These profiles were calculated as follows. For each degree of longitude the average vertical wind profile over one sol (Ls=270°) was calculated. The resulting set of profiles were then averaged to create the zonally sol averaged profile. In addition local, i.e. at each landing site, sol averaged profiles are plotted. This is the vertical wind profile at the longitude and latitude of the landing site averaged over one sol at the winter solstice.

For the VL-1 site the maximum speed determined from the model, as shown in figure 9 (a), is 0.08 m s^{-1} and occurs at an altitude of 16 km above the surface. The maximum vertical wind speed for the sol averaged profile from the MCD at the VL-1 site is -0.11 m s^{-1} and occurs at an altitude of 10 km above the surface. The directions of the vertical wind speeds do not compare well. This may not be surprising as strong westerlies at the latitude will advect heat away or into the region above VL-1 resulting in atmospheric temperature profile that is not directly related to the local diabatic and adiabatic processes.

Figure 7 shows a intense region of down welling air centred around a longitude of -120°E from where the adiabatically generated heat could perhaps be transported to the VL-1 site by advection (Showman et al., 2013). The time taken for an air parcel travelling at 40 m s^{-1} to cover 5400 km distance to the VL-1 site would take about 0.9 sols. This is comparable to the radiative lifetime of the Martian atmosphere of 1-2 sols.

Geosci. Instrum. Method. Data Syst. Discuss., https://doi.org/10.5194/gi-2019-8
Manuscript under review for journal Geosci. Instrum. Method. Data Syst.
Discussion started: 3 April 2019

Geoscientific Instrumentation Methods and Data Systems Discussions
Open Access
EGU

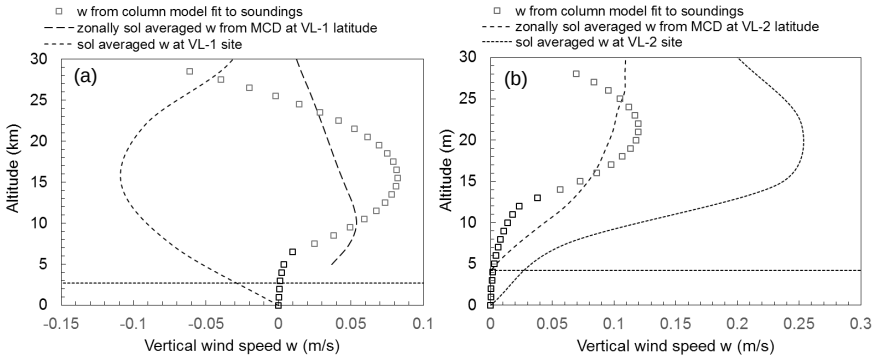

Fig. 9. Comparison of the derived vertical wind speed (positive downward) from the model against the average zonal vertical wind speeds from the MCD for the VL-1 and VL-2 sites at Ls 270°.

The zonally sol averaged temperature, that represents the region to the west of the VL-1 site, is plotted in figure 9 (a). This shows an improved agreement with the model derived vertical wind speed. Here the maximum vertical wind velocity is 0.05 m s^{-1} and occurs at an altitude of 10 km. However this altitude is lower than the model derived profile which may be because the warm advected air is raised to a higher altitude by rising air currents as it approaches the VL-1 site.

For the VL-2 site the maximum speed determined from the model, as shown in figure 9 (b), is 0.12 m s^{-1} and occurs at an altitude of 16 km above the surface. The maximum vertical wind speed for the sol averaged profile from the MCD at the VL-2 site is 0.25 m s^{-1} and occurs at an altitude of 15 km above the surface. The values for the vertical wind speeds do not compare well although the altitude and direction are in close agreement. Again advection is probable playing an important role is this region. However VL-2 appears to be at an latitude where the vertical wind speed and direction are more consistent presumably being less influenced by the topography that helps focus the streams at the latitude of VL-1. Averaging the vertical wind speed then produces quite a good agreement with the model derived vertical wind speed.

6 Concluding remarks

We have described and demonstrated a software application that provides database query and data analysis tools for streamlining investigations of the Martian atmosphere. The main components of the software application include a column model, MCS sounding observations and a software wrapper. The software wrapper uses the Pandas data framework to allow the soundings, stored on a host machine, to be quickly accessed. Searching uses a filter with parameters set using a GUI. The column model is a 1D model that has been extensively used to model the Planetary Boundary Layer.

The column model was initialised with data from the soundings observations and the observed dust properties of the atmosphere at the time of the soundings. Soundings were selected around the

Geosci. Instrum. Method. Data Syst. Discuss., https://doi.org/10.5194/gi-2019-8
Manuscript under review for journal Geosci. Instrum. Method. Data Syst.
Discussion started: 3 April 2019

Geoscientific Instrumentation Methods and Data Systems Discussions
Open Access
EGU

VL-1, VL-2 and MSL landing sites as these are well characterised regions of Mars.

We found the column model usually reproduced the lapse rate and average temperature observed in vertical profiles derived from the Mars Climate Sounder observations. The column model was also found, in the majority of cases, to compare favourably with the Mars Climate Database. Soundings extracted by our software, spanning an area of 5-10 degrees latitude and longitude and over a range in aerocentric longitude of 1-2 degrees, were similar with little difference (<5 K) in temperature between each other in temperature).

We found significant differences between the column model, which essentially represents an atmosphere in radiative equilibrium above the PBL, and the soundings at the VL-1 and VL-2 sites but not at MSL during the winter solstice. We suspect heating of the atmosphere by the meridional Hadley cell circulation down welling over the middle and high latitudes in winter was likely responsible for this mismatch.

A Hill climbing algorithm was used to vary the parameters of an adiabatic heating term added to the column model to fit it to the soundings. We found that the required maximum vertical velocity over the VL-1 site reached a maximum of 8 cm s^{-1} at an altitude of 15 km at Ls 270°. At the VL-2 site the respective maximum vertical velocity was 12 cm s^{-1} at an altitude of 20 km. The model derived vertical velocity profile corresponded significantly better with the zonal average of $w(z)$ obtained from the GCM-based MCD than with $w(z)$ obtained over the landing sites. The fitting approach developed here then provides a way to independantly estimate or 'observe' the vertical motion in the Martian atmosphere.

Future modifications to the framework will likely be the inclusion of a generalized Hill climbing algorithm. This could enable the variation of multiple parameters in the model. This would then enable a fitting temperatures from individual layers in the model to the soundings. Alternatively it could allow the variation of multiple properties, e.g. opacity, wind speed etc., to find a fit between the model and the soundings.

Acknowledgements. AH and HS wishe to acknowledge Finnish Academy grant #310509.

References

Heavens, N. G., McCleese, D. J., Richardson, M. I., Kass, D. M., Kleinböhl, A., and Schofield, J. T.: Structure and dynamics of the Martian lower and middle atmosphere as observed by the Mars Climate Sounder: 2. Implications of the thermal structure and aerosol distributions for the mean meridional circulation, Journal of Geophysical Research (Planets), 116, E01010, 2011.

Holton, J. R.: An introduction to dynamic meteorology, International Geophysics Series, Elsevier Academic Press,, Burlington, MA, 4 edn., 2004.

Joyner, R. and Sayfi, E.: Mars Climate Sounder Derived Data Record (DDR) Software Interface Specification, Tech. rep., 2012.

Kleinböhl, A., Schofield, J. T., Kass, D. M., Abdou, W. A., Backus, C. R., Sen, B., Shirley, J. H., Lawson, W. G., Richardson, M. I., Taylor, F. W., Teanby, N. A., and McCleese, D. J.: Mars Climate Sounder limb profile retrieval of atmospheric temperature, pressure, and dust and water ice opacity, Journal of Geophysical Research (Planets), 114, E10006, 2009.

Lewis, S. R., Collins, M., Read, P. L., Forget, F., Hourdin, F., Fournier, R., Hourdin, C., Talagrand, O., and Huot, J.-P.: A climate database for Mars, Journal of Geophysical Research, 104, 24 177–24 194, 1999.

McCleese, D. J., Schofield, J. T., Taylor, F. W., Calcutt, S. B., Foote, M. C., Kass, D. M., Leovy, C. B., Paige, D. A., Read, P. L., and Zurek, R. W.: Mars Climate Sounder: An investigation of thermal and water vapor structure, dust and condensate distributions in the atmosphere, and energy balance of the polar regions, Journal of Geophysical Research (Planets), 112, E05S06, doi:10.1029/2006JE002790, 2007.

Paton, M. D., Harri, A.-M., Savijärvi, H., Mäkinen, T., Hagermann, A., Kemppinen, O., and Johnston, A.: Thermal and microstructural properties of fine-grained material at the Viking Lander 1 site, Icarus, 271, 360–374, 2016.

Paton, M. D., Harri, A.-M., and Savijärvi, H.: Measurement of Martian boundary layer winds by the displacement of jettisoned lander hardware, Icarus, 309, 345–362, doi:10.1016/j.icarus.2018.03.020, 2018.

Rafkin, S. C. R., Haberle, R. M., and Michaels, T. I.: The Mars Regional Atmospheric Modeling System: Model Description and Selected Simulations, Icarus, 151, 228–256, 2001.

Read, P. L. and Lewis, S. R.: Topographical influences on atmospheric circulation, pp. 73–108, 2004.

Savijärvi, H.: Mars boundary layer modeling: Diurnal moisture cycle and soil properties at the Viking Lander 1 Site., Icarus, 117, 120–127, 1995.

Savijärvi, H.: A model study of the atmospheric boundary layer in the Mars Pathfinder lander conditions., Quarterly Journal of the Royal Meteorological Society, 125, 483–493, 1999.

Savijärvi, H. and Kauhanen, J.: Surface and boundary-layer modelling for the Mars Exploration Rover sites, Quarterly Journal of the Royal Meteorological Society, 134, 635–641, 2008.

Savijärvi, H. and Määttänen, A.: Boundary-layer simulations for the Mars Phoenix lander site, Quarterly Journal of the Royal Meteorological Society, 136, 1497–1505, 2010.

Savijärvi, H., Määttänen, A., Kauhanen, J., and Harri, A.-M.: Mars Pathfinder: New data and new model simulations, Quarterly Journal of the Royal Meteorological Society, 130, 669–683, 2004.

Savijärvi, H., Crisp, D., and Harri, A.-M.: Effects of CO2 and dust on present-day solar radiation and climate on Mars, Quarterly Journal of the Royal Meteorological Society, 131, 2907–2922, 2005.

Savijärvi, H., Paton, M., and Harri, A.-M.: New column simulations for the Viking landers: Winds, fog, frost,

315 adsorption?, Icarus, 310, 48–53, doi:10.1016/j.icarus.2017.11.007, 2018.

Showman, A. P., Wordsworth, R. D., Merlis, T. M., and Kaspi, Y.: Atmospheric Circulation of Terrestrial Exoplanets, pp. 277–326, 2013.

Spiga, A. and Forget, F.: A new model to simulate the Martian mesoscale and microscale atmospheric circulation: Validation and first results, Journal of Geophysical Research (Planets), 114, E02009, 2009.

320 Toigo, A. D. and Richardson, M. I.: A mesoscale model for the Martian atmosphere, Journal of Geophysical Research (Planets), 107, 5049, 2002.

Tyler, D., Barnes, J. R., and Haberle, R. M.: Simulation of surface meteorology at the Pathfinder and VL1 sites using a Mars mesoscale model, Journal of Geophysical Research (Planets), 107, 5018, 2002.

Appendix A MCS sounding information

Geosci. Instrum. Method. Data Syst. Discuss., https://doi.org/10.5194/gi-2019-8
Manuscript under review for journal Geosci. Instrum. Method. Data Syst.
Discussion started: 3 April 2019

Geoscientific Instrumentation Methods and Data Systems Discussions
Open Access
EGU

Table 1. MCS sounding details, thermal inertia and albedo for the VL-1 site.

Date	Time	MY	Ls	LTST	TI	Albedo	latitude	longitude
19.6.2015	04:29:54.870	33	0.33166	0.040692	193	0.21	21.61053	-46.9624
19.6.2015	06:15:02.670	33	0.36806	0.099539	175	0.19	24.13171	-51.3624
19.6.2015	06:16:12.303	33	0.36847	0.098892	205	0.21	20.49613	-51.8776
19.6.2015	06:17:19.887	33	0.36885	0.098409	223	0.21	17.35894	-52.3254
20.6.2015	06:33:24.988	33	0.87268	0.099964	181	0.16	25.5957	-46.1212
19.6.2015	16:52:57.512	33	0.58889	0.536651	229	0.22	18.12454	-49.246
19.6.2015	16:55:55.688	33	0.58992	0.529956	187	0.14	26.75472	-52.3787
20.6.2015	17:14:22.094	33	1.0942	0.531142	181	0.16	25.51972	-46.8809
20.6.2015	18:56:35.820	33	1.12952	0.593921	229	0.22	18.47433	-49.1592
20.6.2015	18:57:43.398	33	1.12991	0.593245	205	0.21	22.18652	-49.6764
23.6.2008	23:49:47.086	29	89.45215	0.139843	229	0.15	26.5135	-48.451
23.6.2008	23:50:11.664	29	89.45227	0.139598	235	0.19	25.23111	-48.639
23.6.2008	23:50:36.234	29	89.4524	0.139365	223	0.21	23.95071	-48.8226
23.6.2008	23:51:00.812	29	89.45252	0.13916	229	0.21	22.76731	-48.996
23.6.2008	23:51:25.391	29	89.45265	0.138932	205	0.21	21.48492	-49.178
24.6.2008	12:13:04.039	29	89.67982	0.634792	247	0.22	17.58154	-51.1372
24.6.2008	12:13:28.613	29	89.67995	0.634321	223	0.21	18.99713	-51.4066
24.6.2008	12:14:17.766	29	89.6802	0.633432	211	0.21	21.63531	-51.926
24.6.2008	12:14:42.340	29	89.68032	0.632977	229	0.21	22.94991	-52.1894
24.6.2008	12:15:06.918	29	89.68045	0.632473	163	0.19	24.36031	-52.4702
2.7.2016	07:55:29.078	33	178.6888	0.082429	181	0.21	23.41032	-51.5822
3.7.2016	08:13:31.006	33	179.2576	0.081776	181	0.16	25.29812	-46.5886
3.7.2016	08:15:48.219	33	179.2585	0.084434	241	0.22	18.64674	-46.188
3.7.2016	09:59:38.203	33	179.2991	0.142427	187	0.16	25.4339	-50.5756
3.7.2016	10:00:47.840	33	179.2995	0.141773	211	0.21	21.79532	-51.0934
4.7.2016	22:42:04.734	33	180.1603	0.635867	211	0.21	20.61232	-48.8378
4.7.2016	22:43:14.367	33	180.1607	0.63516	217	0.19	24.43571	-49.375
5.7.2016	23:00:10.766	33	180.7317	0.63629	229	0.22	18.63573	-43.4714
5.7.2016	23:01:18.344	33	180.7321	0.635617	187	0.21	22.34612	-43.9876
5.7.2016	23:02:27.977	33	180.7326	0.634889	181	0.14	26.1691	-44.532
26.11.2016	07:14:08.021	33	268.7271	0.109216	175	0.19	23.53151	-43.2046
26.11.2016	07:15:17.652	33	268.7276	0.108566	235	0.21	19.89353	-43.721
26.11.2016	09:12:05.891	33	268.7787	0.176737	211	0.21	22.40873	-47.585
27.11.2016	09:32:45.688	33	269.4174	0.172664	235	0.22	17.36794	-44.2724
29.11.2016	08:16:40.131	33	270.6423	0.047931	175	0.19	24.35192	-51.0652
26.11.2016	19:36:25.742	33	269.0518	0.601876	247	0.22	17.48013	-46.3672
26.11.2016	19:36:35.984	33	269.0518	0.601777	241	0.22	18.02713	-46.4444
26.11.2016	19:36:46.227	33	269.0519	0.601682	241	0.22	18.57593	-46.52
26.11.2016	19:36:56.461	33	269.052	0.601585	235	0.21	19.12413	-46.5964
26.11.2016	19:37:25.141	33	269.0522	0.601284	205	0.21	20.75652	-46.8212

Geosci. Instrum. Method. Data Syst. Discuss., https://doi.org/10.5194/gi-2019-8
Manuscript under review for journal Geosci. Instrum. Method. Data Syst.
Discussion started: 3 April 2019

Geoscientific Instrumentation Methods and Data Systems Discussions
Open Access
EGU

Table 2. MCS sounding details, thermal inertia and albedo for the VL-2 site.

Date	Time	MY	Ls	LTST	TI	Albedo	latitude	longitude
18.6.2015	15:14:47.000	33	0.05616	0.015598	289	0.13	48.33603	137.508
20.6.2015	21:27:52.500	33	1.18177	0.209044	319	0.14	49.49605	135.4701
21.6.2015	19:49:45.031	33	1.64491	0.106643	253	0.16	50.22677	132.0431
21.6.2015	19:50:54.664	33	1.64531	0.105401	277	0.13	46.7042	131.3139
21.6.2015	19:52:02.250	33	1.6457	0.104319	289	0.14	43.18882	130.6501
25.6.2008	13:05:58.871	29	90.13729	0.147303	253	0.17	52.86794	130.0865
26.6.2008	13:24:47.762	29	90.58455	0.147361	271	0.14	52.74914	135.1251
26.6.2008	13:25:12.336	29	90.58468	0.146833	295	0.14	51.47195	134.8355
26.6.2008	13:25:36.914	29	90.5848	0.146337	313	0.14	50.19476	134.5571
26.6.2008	13:26:01.484	29	90.58493	0.1459	325	0.14	49.01757	134.3001
2.7.2016	18:58:16.945	33	178.9473	0.050909	271	0.14	52.05622	135.797
2.7.2016	19:00:34.156	33	178.9482	0.062465	295	0.11	46.11084	139.4011
2.7.2016	22:38:22.383	33	179.0331	0.19793	301	0.14	50.52698	135.1719
4.7.2016	21:24:21.461	33	180.1299	0.086136	259	0.16	51.80959	132.1703
5.7.2016	21:42:43.867	33	180.7013	0.08522	277	0.14	52.69278	136.9886
26.11.2016	22:08:39.797	33	269.1183	0.21254	307	0.12	47.36186	136.4497
27.11.2016	20:29:12.703	33	269.7043	0.11631	271	0.14	52.65094	135.7965
27.11.2016	20:30:16.180	33	269.7048	0.115048	319	0.14	49.46057	135.0847
27.11.2016	20:31:25.820	33	269.7053	0.113795	301	0.11	45.831	134.3515
27.11.2016	22:28:14.047	33	269.7563	0.208014	307	0.11	45.63425	139.8646

Geosci. Instrum. Method. Data Syst. Discuss., https://doi.org/10.5194/gi-2019-8
Manuscript under review for journal Geosci. Instrum. Method. Data Syst.
Discussion started: 3 April 2019

Geoscientific Instrumentation Methods and Data Systems Discussions
Open Access
EGU

Table 3. MCS sounding details, thermal inertia and albedo for the Curiosity site.

Date	Time	MY	Ls	LTST	Thermal inertia	Albedo	latitude	longitude
18.6.2015	17:17:54.086	33	0.09883	0.09543	103	0.32	-1.4044	136.285
18.6.2015	17:19:42.633	33	0.09946	0.09462	115	0.2	-6.95597	135.5534
19.6.2015	19:35:09.547	33	0.64501	0.156779	97	0.32	-2.74299	134.527
19.6.2015	19:37:26.766	33	0.6458	0.156064	115	0.19	-9.58537	133.7128
20.6.2015	19:53:44.148	33	1.14926	0.157053	85	0.32	-1.87539	139.6632
23.6.2008	10:52:54.914	29	89.21425	0.135417	451	0.32	-0.5726	138.9962
23.6.2008	10:53:19.484	29	89.21437	0.13522	91	0.32	-1.87	138.8256
23.6.2008	10:53:44.062	29	89.2145	0.135055	79	0.29	-3.07059	138.6664
23.6.2008	10:54:08.641	29	89.21462	0.134855	79	0.27	-4.37039	138.4948
23.6.2008	10:54:33.215	29	89.21475	0.134652	85	0.23	-5.67158	138.322
2.7.2016	19:17:56.586	33	178.9549	0.085568	79	0.29	-4.10859	143.4908
2.7.2016	21:02:54.148	33	178.9959	0.13812	103	0.32	-1.23639	136.8704
2.7.2016	21:04:03.781	33	178.9963	0.137553	85	0.26	-4.92298	136.3838
3.7.2016	21:22:03.664	33	179.5657	0.137972	85	0.3	-2.60699	141.7724
3.7.2016	23:19:30.789	33	179.6116	0.199221	109	0.32	-1.4164	135.243
26.11.2016	22:08:39.797	33	269.1183	0.21254	307	0.12	47.36186	136.4497
27.11.2016	20:29:12.703	33	269.7043	0.11631	271	0.14	52.65094	135.7965
27.11.2016	20:30:16.180	33	269.7048	0.115048	319	0.14	49.46057	135.0847
27.11.2016	20:31:25.820	33	269.7053	0.113795	301	0.11	45.831	134.3515
27.11.2016	22:28:14.047	33	269.7563	0.208014	307	0.11	45.63425	139.8646